Contribution from the Department of Chemistry,
University of Rochester, Rochester, New York 14627

Molecular A Frames. $[Ir_2(\mu\text{-}S)(CO)_2(PPh_2CH_2PPh_2)_2]$, Its Reactions with CO and H_2, and the Structure of Its Carbonyl Adduct

CLIFFORD P. KUBIAK, CARRIE WOODCOCK, and RICHARD EISENBERG*

Received January 30, 1980

The reaction of $[Ir_2Cl(CO)_4(dpm)_2]^+A^-$ (A^- = $[IrCl_2(CO)_2]^-$ or PF_6^-, dpm = bis(diphenylphosphino)methane) with S^{2-} results in the new A-frame complex $[Ir_2(\mu\text{-}S)(CO)_2(dpm)_2]$. This complex reacts with CO to form $[Ir_2(\mu\text{-}S)(\mu\text{-}CO)(CO)_2(dpm)_2]$ which is found by single-crystal X-ray analysis to possess an A-frame type structure with a CO molecule in the endo pocket, bridging the metal centers. The two iridium atoms exhibit square-pyramidal coordination, sharing a common apex at the bridging CO. The Ir–Ir distance is 2.843 (2) Å. The oxidative addition of H_2 to $[Ir_2(\mu\text{-}S)(CO)_2(dpm)_2]$ leads to two different binuclear hydride species, $[Ir_2H_2(\mu\text{-}S)(CO)_2(dpm)_2]$, which are characterized by ^1H NMR and IR spectroscopy. In the presence of H_2, $[Ir_2(\mu\text{-}S)(CO)_2(dpm)_2]$ is found to catalyze the reduction of acetylene, ethylene, and propylene to the corresponding alkane, after which $[Ir_2(\mu\text{-}S)(CO)_2(dpm)_2]$ may be recovered quantitatively.

Introduction

The first binuclear complexes having the A-frame geometry, I, were reported in 1977.[1,2] Since that time, numerous other

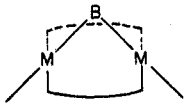

I

reports of A-frame complexes and their reaction chemistry have appeared.[3–15] The focus of many of these studies has been the binding of small molecules, L, in the pocket or endo site of the A-frame complex[3–8]

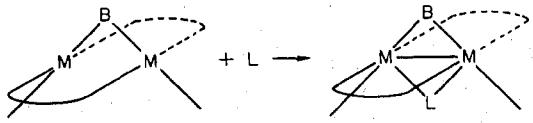

where M = Rh(I), B = S and L = SO_2, B = Cl and L = CO or SO_2, and B = H and L = CO. The goal of these studies is to use the two metal centers of the binuclear A-frame in a cooperative way to activate the added substrate, L, toward subsequent reactions.[1] Several A-frame complexes of Rh(I) have been found to form stable endo adducts with CO and SO_2.[3–7] One of these adducts, $[Rh_2(\mu\text{-}H)(\mu\text{-}CO)(CO)_2(dpm)_2]^+$ (dpm = bis(diphenylphosphino)methane) has proved to be a highly active catalyst for the water gas shift reaction.[4] Others prepared to date, however, show considerable lability of the addendum and little other chemistry besides substrate replacement.[5–7]

Related efforts to protonate or alkylate the A-frame metal centers have, in several cases, been undermined by competitive reactivity of bridgehead ligands. The sulfide-bridged rhodium A frame, $[Rh_2(\mu\text{-}S)(CO)_2(dpm)_2]$, when treated with Et_2OR^+ (R = H, Et) is protonated or alkylated preferentially at sulfur.[1,3] Other attempts in our laboratory of oxidative addition reactions to the metal centers of A-frame complexes have met with similar results. The alkyl halides $PhCH_2Br$, MeI, and EtI react with $[Rh_2(\mu\text{-}S)(CO)_2(dpm)_2]$ at the bridgehead, leading to sulfur alkylation or removal.[1,3] Direct observation of the oxidative addition of hydrogen to an A-frame complex has not been made prior to this report.

In our continuing studies of A-frame molecules, we have prepared $[Ir_2(\mu\text{-}S)(CO)_2(dpm)_2]$. This complex is the iridium analogue of the first reported rhodium A frame, $[Rh_2(\mu\text{-}S)(CO)_2(dpm)_2]$.[1] The reaction chemistry of the iridium species with CO and H_2, however, contrasts sharply with that of its rhodium analogue. We report herein the preparation of the iridium sulfide A-frame complex and the characterization of products obtained in reactions with CO and H_2. The structure of an endo μ-CO adduct, $[Ir_2(\mu\text{-}S)(\mu\text{-}CO)(CO)_2(dpm)_2]$, is established by X-ray crystallography. A dihydrogen oxidative addition product $[Ir_2H_2(\mu\text{-}S)(CO)_2(dpm)_2]$, is characterized by ^1H NMR and is believed to be a symmetrical endo adduct. We also present results of initial studies of the activity of the hydride species as a homogeneous hydrogenation catalyst.

Experimental Section

Materials. Iridium trichloride hydrate (Matthey Bishop), bis(diphenylphosphino)methane (Strem), sodium sulfide hydrate (Mallinckrodt), boron trifluoride–diethyl ether (Eastman), and the gases H_2, D_2, CO, ethylene, propylene, and acetylene (Matheson) were used as purchased. All solvents were reagent grade and dried and degassed before use.

Preparation and Characterization of Complexes. All syntheses were routinely performed under an atmosphere of dry nitrogen by using modified Schlenk techniques. $[Ir_2Cl_2(1,5\text{-}COD)_2]$ (COD = cyclooctadiene) was prepared by a slight modification of a published procedure.[16] Yields of $[Ir_2Cl_2(1,5\text{-}COD)_2]$ were found to be increased by the addition of ca. 10 mL of water at the end of the reaction and removal of ethanol on a rotary evaporator.

Elemental analyses were performed by Galbraith Laboratories, Inc., Knoxville, Tenn. ^1H NMR spectra were recorded on a JEOL JNM-PS-100 Fourier transform spectrometer with ^{31}P spin decoupler.[17] Infrared spectra were recorded on a Perkin-Elmer 467 grating spectrometer calibrated with polystyrene film.[17] Samples were either KBr pellets or Nujol mulls on NaCl plates.

$[Ir_2Cl(CO)_4(PPh_2CH_2PPh_2)_2]^+A^-$ (A^- = $IrCl_2(CO)_2^-$, PF_6^-). $[Ir_2Cl_2(1,5\text{-}COD)_2]$ (0.2 g) and bis(diphenylphosphino)methane (0.3 g) are dissolved in 25 mL of THF. CO gas is bubbled through the solution, and a bright red color develops over ca. 1 min. Continued

(1) Kubiak, C. P.; Eisenberg, R. *J. Am. Chem. Soc.* **1977**, *99*, 6129.
(2) Olmstead, M. M.; Hope, H.; Benner, L. S.; Balch, A. L. *J. Am. Chem. Soc.* **1977**, *99*, 5502.
(3) Kubiak, C. P.; Eisenberg, R. *Inorg. Chem.*, preceding paper in this issue.
(4) Kubiak, C. P.; Eisenberg, R. *J. Am. Chem. Soc.* **1980**, *102*, 3637.
(5) Cowie, M.; Dwight, S. K.; Sanger, A. R. *Inorg. Chim. Acta* **1978**, *31*, L407.
(6) Cowie, M.; Mague, J. T.; Sanger, A. R. *J. Am. Chem. Soc.* **1978**, *100*, 3628.
(7) Mague, J. T.; Sanger, A. R. *Inorg. Chem.* **1979**, *18*, 2060.
(8) Cowie, M.; Dwight, S. K. *Inorg. Chem.* **1979**, *18*, 2700.
(9) Benner, L. S.; Balch, A. L. *J. Am. Chem. Soc.* **1978**, *100*, 6099.
(10) Balch, A. L.; Benner, L. S.; Olmstead, M. M. *Inorg. Chem.* **1979**, *18*, 2996.
(11) Colton, R.; McCormick, M. J.; Pannan, C. D. *J. Chem. Soc., Chem. Commun.* **1977**, 823.
(12) Colton, R.; McCormick, M. J.; Pannan, C. D. *Aust. J. Chem.* **1978**, *31*, 1425.
(13) Brown, M. P.; Puddephatt, R. J.; Rashidi, M.; Seddon, K. R. *Inorg. Chim. Acta* **1977**, *23*, L27.
(14) Brown, M. P.; Fisher, J. R.; Puddephatt, R. J.; Seddon, K. R. *Inorg. Chem.* **1979**, *18*, 2808.
(15) Rattray, A. D.; Sutton, D. *Inorg. Chim. Acta* **1978**, *27*, L85.
(16) Herde, J. L.; Lambert, J. C.; Senott, C. V. *Inorg. Synth.* **1974**, *15*, 18.
(17) For NMR data: s = singlet, d = doublet, t = triplet, quar = quartet, quin = quintet, m = multiplet. For IR data: vs = very strong, s = strong, m = medium, w = weak, sh = shoulder.

0020-1669/80/1319-2733$01.00/0

bubbling of CO causes the color to fade to pale yellow, and after 15 min, a colorless precipitate is obtained. Diethyl ether (10 mL) is added to the solution, and the precipitate is collected (yield ca. 90%). IR: ν(CO) 2048 m, 1998 vs, 1975 s, 1759 s cm^{-1} (Nujol).

The observed physical and chemical characteristics of samples prepared by our procedure above are consistent with those found in a recent report of the BPh_4^- salt of the complex.[7]

The PF_6^- salt is prepared by dissolving $[Ir_2Cl(CO)_4(dpm)_2]^+$-$[IrCl_2(CO)_2]^-$ (0.2 g) in 10 mL of CH_2Cl_2 under a CO atmosphere. A solution of NH_4PF_6 (0.04 g) dissolved in 20 mL of EtOH is then added. CH_2Cl_2 is removed by a CO stream until a precipitate appears. The solution is stored under CO at −10 °C for 24 h to obtain pale yellow microcrystals. Anal. Calcd for $C_{54}H_{44}P_5ClF_6O_4Ir_2$: C, 44.85; H, 3.08; P, 10.73. Found: C, 44.42; H, 3.12; P, 10.68. IR:[17] ν(CO) 2040 m, 1981 vs, 1760 s cm^{-1} (KBr).

$[Ir_2(\mu\text{-}S)(CO)_2(PPh_2CH_2PPh_2)_2]$. $[Ir_2Cl(CO)_4(dpm)_2]^+A^-$ (A = $IrCl_2(CO)_2$ or PF_6) is dissolved in 30 mL of 1:1 CH_2Cl_2–MeOH. A 10% excess of $Na_2S\cdot 9H_2O$ dissolved in 10 mL of MeOH is added, and the solution color becomes orange. The solution is then refluxed at 40 °C under an N_2 stream for 30 min to obtain a purple solution. CH_2Cl_2 is removed on a rotary evaporator to obtain a precipitate which is recrystallized from CH_2Cl_2–MeOH to give deep purple crystals (yield ca. 70%). Anal. Calcd for $C_{52}H_{44}P_4SO_2Ir_2$: C, 50.31; H, 3.55; P, 10.00; S, 2.38. Found: C, 49.91; H, 3.52; P, 10.09; S, 2.65. IR: ν(CO) 1918 s, 1902 vs (Nujol); 1935 s, 1920 vs cm^{-1} (CH_2Cl_2).

$[Ir_2(\mu\text{-}S)(\mu\text{-}CO)(CO)_2(PPh_2CH_2PPh_2)_2]$. $[Ir_2(\mu\text{-}S)(CO)_2(dpm)_2]$ (0.1 g) is partially dissolved in 5 mL of toluene. The solution is placed under an atmosphere of CO, leading within 5 min to a yellow homogeneous solution. Diethyl ether (5 mL) is added, and the solution is stored at −10 °C for 12 h to obtain yellow crystals (yield ca. 90%). The crystals so obtained contain two solvent toluene molecules per molecule of complex. Anal. Calcd for $C_{67}H_{60}P_4SO_3Ir_2$: C, 55.36; H, 4.16; P, 8.52; S, 2.21. Found: C, 55.06; H, 4.28; P, 8.19; S, 2.54. IR: ν(CO) 1953 s, 1965 vs, 1760 s (Nujol); 1937 vs, 1950 s, 1725 s cm^{-1} (toluene).

Reaction of $[Ir_2(\mu\text{-}S)(\mu\text{-}CO)(CO)_2(PPh_2CH_2PPh_2)_2]$ with BF_3. Preparation of $[Ir_2(\mu\text{-}S)(BF_3)(CO)_2(PPh_2CH_2PPh_2)_2]$. $[Ir_2(\mu\text{-}S)(\mu\text{-}CO)(CO)_2(dpm)_2]$ (0.1 g) is dissolved in 15 mL of THF under CO. Boron trifluoride–diethyl ether (1–2 drops) is added to give, after cooling to −10 °C for 3 h, a pale yellow precipitate (yield ca. 90%). Anal. Calcd for $C_{52}H_{44}P_4SO_2BF_3Ir_2$: C, 47.70; H, 3.36; P, 9.48; S, 2.45. Found: C, 47.64; H, 3.80; P, 9.24; S, 2.27. IR: ν(CO) 1971 vs, 1990 s cm^{-1} (Nujol).

Reaction of $[Ir_2(\mu\text{-}S)(CO)_2(PPh_2CH_2PPh_2)_2]$ with H_2. Spectroscopic Characterization of $[Ir_2H_2(\mu\text{-}S)(CO)_2(PPh_2CH_2PPh_2)_2]$. $[Ir_2(\mu\text{-}S)(CO)_2(dpm)_2]$ (0.1 g) is dissolved in 5 mL of toluene at 85 °C under a hydrogen atmosphere. On being cooled to room temperature, the solution turns orange. The IR spectrum was monitored over a period of 6 h, and the following changes were noted. IR (toluene solution, approximate time after solution had cooled to 25 °C): after 5 min, ν(CO) 2006 s, 1921 s; after 1 h, ν(CO) 2006 s, 1960 m, 1921 s; after 6 h, ν(CO) 2006 m, 1976 m, sh, 1960 vs, 1921 s; after >6 h, no significant changes of the spectrum were observed. Repeating the procedure above, but with deuterium gas, leads to the same IR absorptions, verifying their assignment as ν(CO). IR absorptions which could be attributed to Ir–H or Ir–D are not observed. The ^1H NMR spectrum of the species in solution was obtained by repeating the procedure above with H_2 and benzene-d_6 at 75 °C. ^1H NMR (ppm relative to internal Me_4Si, intensity in parentheses):[17] after 1 h, $\delta(C_6H_5)$ 6.67–7.62 m (40), $\delta(CH_2)$ 5.16 m (1.39), 4.63 m (0.61), and 2.57 (two overlapped multiplets, 2.0), δ(H) −10.50 m and −10.79 quin (total integrated intensity for both peaks, 2.0); after 6 h, $\delta(C_6H_5)$ 6.67–7.62 m (40), $\delta(CH_2)$ 5.16 m (0.75), 4.63 m (1.25), and 2.57 (overlapped multiplets, 2.0), δ(H) −10.50 t of t and −10.79 quin (2.0, total). $^1H\{^{31}P\}$ NMR $\delta(CH_2)$ 5.16 d (J_{HH} = 12 Hz), 4.63 d (J_{HH} = 14 Hz), and 2.57 (two overlapped doublets), δ(H) −10.50 s and −10.79 s. Removal of H_2 under vacuum followed by heating at 85 °C under N_2 for 20 min leads to quantitative recovery of the purple starting material, $[Ir_2(\mu\text{-}S)(CO)_2(dpm)_2]$.

Homogeneous Hydrogenations. In a typical experiment, 0.05 g of $[Ir_2(\mu\text{-}S)(CO)_2(dpm)_2]$ was dissolved in 25 mL of toluene in a 100-mL side arm flask stoppered with a "Suba-Seal" (Gallenkamp Ltd.). The flask was charged with ca. 300 torr of H_2 and 300 torr of acetylene, ethylene, propylene, or CO. The flask was then heated to 80 °C, and gases were sampled by using a "Pressure-Lok" gas syringe (Precision Sampling Corp.) and analyzed by GC (Hewlett-Packard 5700A) using a 12-ft Porapak Q column at 43 or 150 °C. GC peak heights for the product and reagent gases were converted to partial pressures by using calibration plots previously obtained. Methane gas (ca. 40 torr) was used as internal calibrant.

Data Collection and Reduction. Yellow crystals of $[Ir_2(\mu\text{-}S)(\mu\text{-}CO)(CO)_2(dpm)_2]\cdot 2C_6H_5CH_3$ were obtained as above. Due to their rapid decomposition with loss of both CO and solvent, a suitable single crystal was mounted quickly on a glass fiber and coated with a layer of epoxy. On the basis of precession photographs it was determined that the crystals belong to the orthorhombic system. The observed systematic absences of $0kl$, $k + l = 2n + 1$, and $h0l$, $h + l = 2n + 1$, are consistent with space groups *Pnnm* (D_{2h}^{12}) and *Pnn*2 (C_{2v}^{10}).[18] The lattice constants at 22 °C were determined from a least-squares refinement of 12 intense, high-angle reflections ($(\sin\theta)/\lambda \geq 0.2368$).[19] These reflections were carefully centered, by using Mo Kα radiation (λ = 0.7093 Å), on a Picker FACS-1 diffractometer equipped with a graphite monochromator. The lattice constants are a = 18.174 (10), b = 23.100 (13), and c = 14.345 (8) Å. The calculated density (Z = 4) of 1.60 g/cm^3 agrees with a value of 1.61 (1) g/cm^3 determined by the flotation method.

The mosaicity of the crystal used for intensity measurements was examined by means of a narrow-source, open-counter ω-scan technique.[20] The full widths at half-maximum for typical strong reflections were ≤0.15°. Intensities were measured by the θ–2θ scan technique. The crystal was mounted with the a^* axis offset by 4.8° from the ϕ axis of the diffractometer. The takeoff angle for the X-ray tube was 1.7°. The scan was from 0.6° below the Kα_1 peak to 0.6° above the Kα_2 peak. The scan speed was 1°/min, and backgrounds were counted at each end of the scan range for 10 s ($2\theta \leq 35°$) or 20 s ($35° < 2\theta \leq 45°$). Attenuator foils were automatically inserted when the intensity of the diffracted beam reached 10 000 counts/s. The pulse-height analyzer was set for a 90% window centered on Mo Kα radiation.

Data were collected from the octant with h, k, and $l \geq 0$ in the range $3.5° \leq 2\theta \leq 45°$. Three standard reflections were monitored every 100 observations. The intensities of the standards varied by less than ±5% over the course of data collection. A total of 4439 reflections were observed. The value of I and $\sigma^2(I)$ were obtained by using expressions described previously[21] and converted to F^2 and $\sigma^2(F^2)$ by application of Lorentz and polarization corrections. The value of p used in the expression for the variance was 0.04.[22] The linear absorption coefficient for Mo Kα radiation is 48.61 cm^{-1}. No correction for absorption was made because of our inability to accurately measure the epoxy-coated crystal. The approximate size of the crystal was 0.3 × 0.3 × 0.4 mm. The final data set consisted of 4439 independent reflections of which 3233 had $F_o^2 \geq 3\sigma(F_o^2)$.

Solution and Refinement of the Structure. The structure was solved by standard heavy-atom methods in the space group *Pnnm*.[23] The position of the iridium atom was determined from a three-dimensional Patterson map. Refinement of the scale factor and atomic positional parameters for the iridium atom resulted in residuals of R_1 = 0.300 and R_2 = 0.411.[24] In this and all subsequent refinements, the quantity minimized was $\sum w(|F_o| - |F_c|)^2$, where the weights, w, were $4F^2/\sigma^2(F^2)$. Only those reflections with $F_o^2 \geq 3\sigma(F_o^2)$ were included in the refinements. Scattering factors for neutral Ir, S, P, C, and O were those tabulated by Cromer and Mann.[25] The effects of anomalous dispersion were included in the calculation of $|F_c|$; values of $\Delta f'$ and $\Delta f''$ were

(18) "International Tables for X-ray Crystallography"; Kynoch Press: Birmingham, England, 1960; Vol. I, pp 120, 146.
(19) The programs for refinement of lattice constants and automated operation of the diffractometer are those of Busing and Levy as modified by Picker Corp.
(20) Furnas, T. C. "Single Crystal Orienter Instruction Manual"; General Electric Co.: Milwaukee, Wis., 1957; Chapter 10.
(21) Goldberg, S. Z.; Kubiak, C.; Meyer, C. D.; Eisenberg, R. *Inorg. Chem.* **1975**, *14*, 1650.
(22) Corfield, P. W. R.; Doedens, R. J.; Ibers, J. A. *Inorg. Chem.* **1967**, *6*, 197.
(23) All computations were performed on an IBM computer. The data processing program was an extensively modified version of Raymond's URFACS. In addition, local versions of the following were used: Ibers' NUCLS, a group least-squares program; Zalkin's FORDAP Fourier program; ORFFE, a function and error program by Busing, Martin, and Levy; Johnson's ORTEP thermal ellipsoid plotting program.
(24) $R_1 = \sum||F_o| - |F_c||/\sum|F_o|$; $R_2 = [\sum w(|F_o| - |F_c|)^2/\sum w|F_o|^2]^{1/2}$. The estimated standard deviation of an observation of unit weight is given by $[\sum w(|F_o| - |F_c|)^2/(N_o - N_v)]^{1/2}$, where N_o and N_v are the number of observations and variables, respectively.
(25) Cromer, D. T.; Mann, B. *Acta Crystallogr., Sect. A* **1968**, *A24*, 321.

Table I. Final Positional and Thermal Parameters for $[Ir_2(\mu\text{-}S)(\mu\text{-}CO)(CO)_2(dpm)_2]\cdot 2C_7H_8$

	x	y	z	β_{11}[a]	β_{22}	β_{33}	β_{12}	β_{13}	β_{23}
Ir	0.115032 (23)[b]	−0.154865 (17)	0.099081 (28)	0.161 (3)	0.084 (1)	0.340 (4)	−0.015 (1)	−0.009 (2)	0.004 (1)
S	0.01933 (22)	−0.11118 (18)	0.0 (0)	0.177 (14)	0.112 (9)	0.477 (25)	0.021 (9)	0.0 (0)	0.0 (0)
P(1)	0.03774 (16)	−0.23479 (12)	0.10615 (21)	0.174 (10)	0.097 (6)	0.386 (17)	−0.016 (6)	0.004 (11)	0.016 (8)
P(2)	0.16872 (16)	−0.06386 (12)	0.10555 (21)	0.195 (10)	0.096 (6)	0.386 (17)	−0.008 (6)	−0.022 (11)	−0.003 (8)
C(1)	0.1530 (7)	−0.1722 (5)	0.2119 (10)	0.27 (5)	0.142 (28)	0.60 (9)	−0.05 (3)	0.06 (6)	0.02 (4)
O(1)	0.1749 (7)	−0.1819 (5)	0.2863 (8)	0.70 (6)	0.37 (3)	0.62 (7)	−0.16 (4)	−0.33 (6)	0.24 (4)
C(2)	0.1862 (9)	−0.1882 (7)	0.0 (0)	0.19 (6)	0.08 (3)	0.47 (10)	−0.04 (4)	0.0 (0)	0.0 (0)
O(2)	0.2425 (6)	−0.2138 (5)	0.0 (0)	0.18 (4)	0.124 (25)	0.58 (8)	0.037 (26)	0.0 (0)	0.0 (0)
C(3)	−0.0170 (8)	−0.2470 (7)	0.0 (0)	0.14 (5)	0.13 (4)	0.33 (9)	−0.03 (3)	0.0 (0)	0.0 (0)
C(4)	0.1549 (9)	−0.0208 (6)	0.0 (0)	0.31 (6)	0.08 (3)	0.26 (8)	0.05 (4)	0.0 (0)	0.0 (0)

[a] The form of the anisotropic thermal ellipsoid is $\exp[-(h^2\beta_{11} + k^2\beta_{22} + l^2\beta_{33} + 2hk\beta_{12} + 2hl\beta_{13} + 2kl\beta_{23})]$. The values have been multiplied by 10^2. [b] The numbers in parentheses in this and in succeeding tables correspond to estimated standard deviations in the least significant figures.

Table II. Group Parameters for $[Ir_2(\mu\text{-}S)(\mu\text{-}CO)(CO)_2(dpm)_2]\cdot 2C_7H_8$[a]

	x_c	y_c	z_c	ϕ	θ	ρ
P(1)C(1)	0.1130 (3)	−0.359 30 (24)	0.1405 (4)	−1.135 (4)	3.099 (5)	0.149 (5)
P(1)C(2)	−0.0824 (4)	−0.231 66 (23)	0.2705 (5)	−1.472 (7)	−2.427 (5)	1.658 (7)
P(2)C(1)	0.1166 (3)	0.021 23 (27)	0.2694 (5)	−2.247 (7)	−2.466 (5)	1.877 (7)
P(2)C(2)	0.3442 (3)	−0.059 02 (27)	0.1350 (4)	0.043 (5)	3.042 (6)	0.128 (5)
T(1)	0.1595 (5)	0.402 5 (4)	0.0 (0)	0.0 (0)	1.57080 (0)	−4.124 (6)
T(2)	0.2293 (8)	−0.355 8 (5)	0.50000 (0)	−1.57080 (0)	−1.57080 (0)	−1.379 (9)

[a] x_c, y_c, and z_c are group center of mass coordinates; ϕ, θ, and ρ are angular parameters described previously;[28] $B = 0.0$ Å^2 is the group thermal parameter which was not refined.

those of Cromer and Liberman.[26] The scattering factors for hydrogen were those of Stewart et al.[27]

A difference Fourier synthesis phased by the iridium atom revealed the positions of two phosphorus atoms and a sulfur atom situated on the mirror plane $x, y, 0$ of the space group *Pnnm*. A difference Fourier synthesis phased by the four atoms Ir, S, P(1), and P(2) revealed the positions of all other nonhydrogen atoms in the molecule. In the refinements which followed, the phenyl rings were treated as rigid groups with d(C–C) = 1.392 Å.[28] Refinement of a model in which all nongroup atoms were given isotropic temperature factors resulted in $R_1 = 0.116$ and $R_2 = 0.178$. A subsequent difference Fourier revealed two toluene molecules of crystallization, each with crystallographic m symmetry, which were expected from results of the density determination and microanalysis. The toluenes were treated as rigid groups with d(C–C) = 1.392 Å and d(CH_3–C) = 1.530 Å. A model in which all nongroup atoms were refined with anisotropic thermal parameters led to $R_1 = 0.055$ and $R_2 = 0.074$. In the final model, dpm phenyl hydrogen atoms were included in the rigid groups with isotropic thermal parameters constrained to $B_H = B_C + 1$. The total of 141 variables for 3233 observations was refined to convergence with residuals of $R_1 = 0.052$ and $R_2 = 0.069$. In the final cycle of refinement, no parameters shifted by more than 13% of their estimated standard deviations. The final estimated standard deviation for an observation of unit weight was 2.50 e. Analysis of the residuals, R_1 and R_2, and the weighting scheme indicates that the weights given to reflections with low values of F_o were overestimated. The relatively high error in an observation of unit weight is attributed to the overweighting of these weak reflections. No other trends in R_1, R_2, or $\sum w(|F_o| - |F_c|)^2$ were apparent, and no change in our original weighting scheme was made since it satisfactorily accounted for all other classes of reflections. The largest peak of a final difference Fourier map was 1.4 e/Å^3 or 40% of a typical carbon atom peak in this study.

The final atomic positional and thermal parameters are given in Table I. Group parameters are given in Table II. Derived positional and thermal parameters for the group atoms are given in Table III. A listing of observed and calculated structure factors is available.

Results and Discussion

The binuclear iridium complex, $[Ir_2Cl(CO)_4(dpm)_2]^+$, is prepared from $[Ir_2Cl_2(1,5\text{-}COD)_2]$, dpm, and CO. The hexafluorophosphate salt exhibits ν(CO) of 2040 m, 1981 vs, and 1760 s cm^{-1} (IBr), and microanalytical data are consistent with the formulation $[Ir_2Cl(CO)_4(dpm)_2]^+PF_6^-$. Mague and Sanger have recently reported the synthesis and characterization of the tetraphenylborate salt.[7] Their physical and chemical observations regarding $[Ir_2Cl(CO)_4(dpm)_2]^+BPh_4^-$, notably, extreme sensitivity to CO loss, are in agreement with our own observations for the $[IrCl_2(CO)_2]^-$ and PF_6^- salts.

$[Ir_2Cl(CO)_4(dpm)_2]^+$ is a convenient starting material for the synthesis of iridium A-frame complexes. Its reaction with S^{2-} leads to the sulfide-bridged A frame, $[Ir_2(\mu\text{-}S)(CO)_2(dpm)_2]$, which exhibits physical properties similar to those found for its rhodium analogue, $[Rh_2(\mu\text{-}S)(CO)_2(dpm)_2]$,[1,3] including two low-energy terminal ν(CO) at 1918 s and 1902 vs cm^{-1} (Nujol). The complex is purple. The chemistry of the iridium species with CO and H_2, however, differs markedly from $[Rh_2(\mu\text{-}S)(CO)_2(dpm)_2]$.

The iridium sulfide A-frame, $[Ir_2(\mu\text{-}S)(CO)_2(dpm)_2]$, reacts rapidly with CO to form an adduct, $[Ir_2(\mu\text{-}S)(\mu\text{-}CO)(CO)_2(dpm)_2]$. This complex displays terminal ν(CO) at 1950 s, 1937 vs, and a relatively low-energy band at 1760 s cm^{-1} (Nujol) corresponding to a bridging carbonyl stretch. The structure of $[Ir_2(\mu\text{-}S)(\mu\text{-}CO)(CO)_2(dpm)_2]$, which has been determined by an X-ray crystallographic study, is described fully below. The complex possesses the structural arrangement of an endo CO adduct of $[Ir_2(\mu\text{-}S)(CO)_2(dpm)_2]$. The addition of CO to the iridium sulfur A frame (eq 1) (dpm ligands not

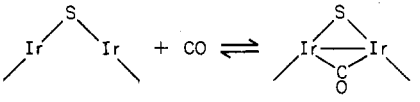

(1)

shown) is similar to reactions of the cationic μ-H or μ-Cl rhodium A frames (eq 2).[4,5] An intriguing property of the

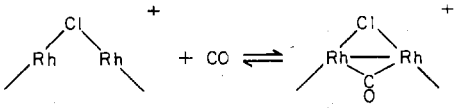

(2)

neutral iridium complex is that its carbonyl stretching frequency appears approximately 100 cm^{-1} lower in energy than the related rhodium systems, suggesting a reduction in the C–O bond order. We have attempted to probe the reactivity of the

(26) Cromer, D. T.; Liberman, D. *J. Chem. Phys.* **1970**, *53*, 1891.
(27) Stewart, R. F.; Davidson, E. R.; Simpson, W. T. *J. Chem. Phys.* **1965**, *42*, 3175.
(28) Eisenberg, R.; Ibers, J. A. *Inorg. Chem.* **1965**, *4*, 773. LaPlaca, S. J.; Ibers, J. A. *J. Am. Chem. Soc.* **1965**, *87*, 2851; *Acta Crystallogr.* **1965**, *18*, 511.
(29) Taylor, R. C.; Young, J. F.; Wilkinson, G. *Inorg. Chem.* **1966**, *5*, 20.

Table III. Derived Positional and Thermal Parameters of the Group Atoms[a]

	x	y	z	B, Å²
		C(1)		
P(1)C(11)	0.0806 (4)	−0.30545 (27)	0.1260 (6)	2.80 (22)
P(1)C(12)	0.0367 (3)	−0.3544 (4)	0.1368 (6)	4.9 (3)
P(1)C(13)	0.0691 (5)	−0.40825 (29)	0.1513 (7)	6.0 (4)
P(1)C(14)	0.1454 (5)	−0.41315 (27)	0.1549 (7)	5.6 (3)
P(1)C(15)	0.1893 (3)	−0.3642 (4)	0.1441 (6)	4.8 (3)
P(1)C(16)	0.1569 (4)	−0.31036 (29)	0.1297 (6)	3.34 (24)
P(1)H(12)	−0.0153 (3)	−0.3511 (5)	0.1344 (9)	5.9
P(1)H(13)	0.0392 (6)	−0.4417 (4)	0.1586 (10)	7.0
P(1)H(14)	0.1676 (6)	−0.4499 (3)	0.1647 (10)	6.6
P(1)H(15)	0.2413 (3)	−0.3676 (5)	0.1466 (19)	5.5
P(1)H(16)	0.1868 (5)	−0.2770 (4)	0.1223 (9)	4.34
		C(2)		
P(1)C(21)	−0.0320 (4)	−0.2330 (3)	0.1975 (5)	2.93 (23)
P(1)C(22)	−0.1071 (5)	−0.2362 (4)	0.1789 (5)	4.8 (3)
P(1)C(23)	−0.1575 (4)	−0.2349 (4)	0.2519 (6)	5.9 (4)
P(1)C(24)	−0.1329 (5)	−0.2303 (4)	0.3435 (6)	5.2 (3)
P(1)C(25)	−0.0578 (5)	−0.2271 (4)	0.3621 (5)	7.0 (4)
P(1)C(26)	−0.0074 (4)	−0.2285 (4)	0.2891 (6)	5.5 (3)
P(1)H(22)	−0.1239 (6)	−0.2393 (6)	0.1164 (5)	5.8
P(1)H(23)	−0.2087 (4)	−0.2371 (6)	0.2392 (9)	6.9
P(1)H(24)	−0.1673 (6)	−0.2294 (6)	0.3933 (7)	6.2
P(1)H(25)	−0.0410 (7)	−0.2240 (7)	0.4246 (5)	8.0
P(1)H(26)	0.0439 (4)	−0.2263 (6)	0.3018 (8)	6.5
		C(1)		
P(2)C(11)	0.1378 (5)	−0.0155 (3)	0.1973 (5)	3.30 (25)
P(2)C(12)	0.0868 (5)	0.0284 (4)	0.1808 (5)	4.27 (28)
P(2)C(13)	0.0657 (5)	0.0651 (3)	0.2529 (7)	5.8 (4)
P(2)C(14)	0.0954 (6)	0.0579 (4)	0.3416 (6)	6.8 (4)
P(2)C(15)	0.1464 (5)	0.0141 (4)	0.3581 (5)	7.1 (4)
P(2)C(16)	0.1675 (5)	−0.0226 (4)	0.2859 (6)	5.6 (3)
P(2)H(12)	0.0665 (7)	0.0332 (5)	0.1202 (6)	5.27
P(2)H(13)	0.0309 (6)	0.0950 (5)	0.2417 (10)	6.8
P(2)H(14)	0.0810 (8)	0.0829 (5)	0.3908 (7)	7.8
P(2)H(15)	0.1667 (8)	0.0092 (6)	0.4186 (6)	8.1
P(2)H(16)	0.2023 (6)	−0.0525 (5)	0.2972 (9)	6.6
		C(2)		
P(2)C(21)	0.2684 (3)	−0.0623 (4)	0.1227 (6)	2.97 (23)
P(2)C(22)	0.3091 (4)	−0.11256 (28)	0.1372 (6)	4.04 (27)
P(2)C(23)	0.3850 (4)	−0.1092 (3)	0.1494 (7)	5.2 (3)
P(2)C(24)	0.4201 (3)	−0.0557 (4)	0.1472 (7)	5.6 (3)
P(2)C(25)	0.3793 (5)	−0.0053 (3)	0.1328 (7)	6.7 (4)
P(2)C(26)	0.3035 (5)	−0.00880 (29)	0.1205 (6)	5.4 (3)
P(2)H(22)	0.2852 (6)	−0.1491 (3)	0.1387 (9)	5.04
P(2)H(23)	0.4128 (6)	−0.1435 (4)	0.1593 (10)	6.2
P(2)H(24)	0.4719 (4)	−0.0534 (6)	0.1556 (10)	6.6
P(2)H(25)	0.4033 (7)	0.0311 (4)	0.1313 (10)	7.7
P(2)H(26)	0.2757 (6)	0.0255 (4)	0.1106 (9)	6.4
		T(1)		
T(1)C(1)	0.2020 (5)	0.3524 (4)	0.0	4.1 (4)
T(1)C(2)	0.1808 (5)	0.3775 (4)	0.08404 (0)	5.3 (3)
T(1)C(3)	0.1383 (5)	0.4276 (4)	0.08404 (0)	5.7 (3)
T(1)C(4)	0.1170 (7)	0.4527 (5)	0.0	7.2 (6)
T(1)CM	0.2488 (8)	0.2973 (5)	0.0	5.7 (5)
		T(2)		
T(2)C(1)	0.1541 (8)	−0.3444 (6)	0.5	8.9 (8)
T(2)C(2)	0.1917 (8)	−0.3501 (5)	0.41596 (0)	8.8 (6)
T(2)C(3)	0.2669 (8)	−0.3616 (6)	0.41596 (0)	9.7 (6)
T(2)C(4)	0.3045 (8)	−0.3673 (8)	0.5	8.7 (8)
T(2)CM	0.0715 (8)	−0.332 (1)	0.5	15 (1)

[a] In the numbering scheme for phenyl carbons, the first number following P or T identifies the phosphorus atom or toluene to which the ring belongs. For phosphine phenyl rings the first number following C is an identifier for the two phenyl rings bound to the phosphorus atom. The last number always denotes the position of the carbon in the ring with C1 bound to phosphorus or CM, the toluene methyl carbon.

bridging carbon monoxide in $[Ir_2(\mu\text{-}S)(\mu\text{-}CO)(CO)_2(dpm)_2]$ toward Lewis acids. The reaction of $[Ir_2(\mu\text{-}S)(\mu\text{-}CO)(CO)_2(dpm)_2]$ with BF_3, however, leads to loss of CO, as evidenced by only terminal ν(CO) 1971 vs and 1990 s cm^{-1} (Nujol) and microanalytical data which suggest the identity of the product is $[Ir_2(\mu\text{-}S)(BF_3)(CO)_2(dpm)_2]$. It is likely that the bridgehead sulfide serves as the repository for BF_3 in this reaction, much as electrophilic attack by H^+ and Et^+ is found to occur at the sulfide in $[Rh_2(\mu\text{-}S)(CO)_2(dpm)_2]$.[3]

$[Ir_2(\mu\text{-}S)(CO)_2(dpm)_2]$ is the first A-frame complex for which the oxidative addition of hydrogen has been observed directly. The complex adds H_2 in solutions which are heated briefly. IR and NMR data suggest that at least two different binuclear hydride complexes are present in solution and that they slowly interconvert. The IR data indicate that the initial product of the reaction with H_2 is characterized by ν(CO) of 2006 s and 1921 s and that the second species is produced slowly over a period of ca. 6 h. The second species displays ν(CO) of 1976 m, sh and 1960 vs cm^{-1}, and after 6 h the relative intensity of this set of bands is greater than the set of two at 2006 m and 1921 s cm^{-1}. The ^1H NMR data support the conclusion that two hydride species are present in solution and provide information regarding their possible structures. After short reaction times of ca. 1–2 h, the upfield hydride region of the NMR spectrum shows two multiplets which are centered at δ −10.50 and −10.79. The spectrum is shown in Figure 4. The more intense of the two hydride signals is a symmetric 1:4:6:4:1 quintet ($^2J_{H-P}$ = 5.5 Hz). The multiplicity of the resonance at δ −10.50 cannot yet be determined. After longer reaction times, however, the quintet at δ −10.79 loses intensity relative to the second multiplet. The previously unresolved multiplet at δ −10.50 emerges as a triplet of triplets ($^2J_{P-H}$ = 16.1, $^3J_{P-H}$ = 9.0 Hz). The upfield ^1H NMR spectrum, after 12 h, is shown in Figure 5 with an idealized triplet of triplets on the assumption that $^2J_{P-H}$ = 16.1 and $^3J_{P-H}$ = 9.0 Hz. The high-field portion overlaps the now weaker quintet at δ −10.79.

The dpm methylene region of the ^1H NMR is also used to characterize the two different hydride complexes. Each hydride species exhibits its own dpm methylene AB doublet of doublets with superimposed phosphorus coupling. The dpm methylene spectrum after 6 h appears in Figure 6. Phosphorus decoupling confirms the underlying doublet structure of each of the methylene resonances, and two overlapping doublets can be clearly seen at δ 2.57. The phosphorus decoupled hydride resonances appear as singlets (δ −10.50, −10.79).

The relative intensities of the different dpm methylene and Ir hydride resonances change in a parallel fashion. Thus, methylene multiplets at δ 5.16 and 2.57 (overlapped) are assigned to the hydride species I which shows the quintet at δ −10.79; and those at δ 4.59 and 2.57 (overlapped) are assigned to species II which is characterized by a triplet of triplets at δ −10.50. Importantly, the ratio of the total integrated intensity of the methylene region to hydride region remains a constant, 4:2, independent of the relative proportion of I to II. This demonstrates one molecule of H_2 is added to $[Ir_2(\mu\text{-}S)(CO)_2(dpm)_2]$ in both species I and II. Moreover, the symmetric quintet and triplet of triplets hydride signals for I and II indicate the two hydrogen atoms are in both cases equivalent and coupled to all four dpm phosphorus nuclei. The quintet resonance suggests that in I the four phosphorus nuclei are also equivalent.

Possible structures for the hydrogen oxidative addition products, $[Ir_2(\mu\text{-}S)(H_2)(CO)_2(dpm)_2]$, are shown by a–c.

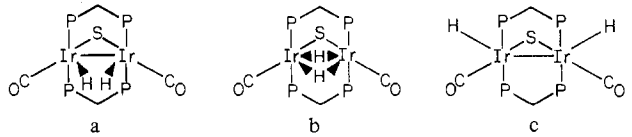

a b c

Each of the structures, a–c, should give rise to a triplet of triplets. The Ir–Ir bond joining the formally Ir(II) centers

in the endo and exo H_2 adducts a and c provides a means for longer range coupling, ($^3J_{P-H}$), which is superimposed on a first-order triplet from coupling ($^2J_{P-H}$) to the two vicinal phosphines cis to each hydride. The observed value of $^2J_{P-H}$, 16.1 Hz, for hydride species II is in the range normally seen for an iridium hydride mutually cis to two phosphines. An alternative to the Ir–Ir bonded structure a is b in which the metals are joined by two bridging hydrides. Again each equivalent hydride would be coupled to two different pairs of phosphorus nuclei. It is not possible to distinguish which of the structures a–c belong to the iridium hydrides I and II. A reasonable proposal, however, is that the quintet hydride resonance exhibited by I represents equilibration between structures a and b. Intramolecular exchange of the two terminal hydrides in a through the formation of the hydride-bridged structure b is the simplest description which accounts for the equivalence of the four phosphorus nuclei to the hydrides. In contrast, the exo hydrides in c no longer have access to the pocket between the iridium centers, and intramolecular exchange would not be expected to be facile. The triplet of triplets displayed by II is therefore attributed to the expectedly static structure c. Low-temperature NMR studies are needed to obtain a more detailed description of the hydrides formed by the oxidative addition of H_2 to $[Ir_2(\mu\text{-}S)(CO)_2(dpm)_2]$ and will be a subject of future investigations.

We have begun to investigate the activity of the hydride species $[Ir_2H_2(\mu\text{-}S)(CO)_2(dpm)_2]$ in homogeneous hydrogenations. Solutions of $[Ir_2(\mu\text{-}S)(CO)_2(dpm)_2]$ under 300 torr of H_2 and an equal pressure of acetylene, ethylene, or propylene reduce the substrate to the saturated product. The rates of production of ethane or propane are 1.2, 6.7, and 2.9 mol of product mol^{-1} of complex h^{-1}, respectively, for acetylene, ethylene, and propylene at 80 °C. In all cases, the iridium sulfide A frame can be recovered quantitatively at the end of the run after heating of the solution under nitrogen.

The proven ability of $[Ir_2(\mu\text{-}S)(CO)_2(dpm)_2]$ to separately add either CO or H_2 suggests the possibility of using both these substrates in catalytic reductions. We have examined the feasibility of hydroformylations and CO reductions, without success to date. For instance, solutions of $[Ir_2(\mu\text{-}S)(CO)_2(dpm)_2]$ under equal pressures of H_2, CO, and C_2H_4 at 80 °C produce ethane, although at a slower rate than with H_2 and C_2H_4 alone. No aldehyde or other oxygenates are detected by IR and GC. Solutions under H_2 and CO show neither gas consumption nor product formation within our limits of detectability up to 105 °C and 1 atm total pressure. It appears that the variation of temperature alone may be insufficient for creating conditions where additional catalytic functions of the complex are operative. Specifically, at higher temperatures and 1 atm pressure the equilibria between $[Ir_2(\mu\text{-}S)(CO)_2(dpm)_2]$, H_2, and CO are observed to favor the separated molecules. Higher and a more varied range of pressures may enable the observation of additional homogeneous reductions catalyzed by the iridium sulfide A frame. We are continuing our investigations along these lines.

Solid-State Structure of $[Ir_2(\mu\text{-}S)(\mu\text{-}CO)(CO)_2(dpm)_2]\cdot 2C_7H_9$. The crystal structure is composed of discrete molecules of $[Ir_2(\mu\text{-}S)(\mu\text{-}CO)(CO)_2(dpm)_2]$ with solvent toluene molecules filling the otherwise void space between. The asymmetric unit contains half of the complex. The present structure is the first determined for an Ir A-frame complex or derivative.

The molecular structure of $[Ir_2(\mu\text{-}S)(\mu\text{-}CO)(CO)_2(dpm)_2]$ consists of two iridium atoms bridged by two bis(diphenylphosphino)methane ligands, a sulfur atom, and carbon monoxide. The bridging sulfur and carbonyl atoms and the dpm methylene carbon atoms lie on a crystallographic mirror plane at $z = 0$. Each $[Ir_2(\mu\text{-}S)(\mu\text{-}CO)(CO)_2(dpm)_2]$ molecule therefore possesses mirror symmetry. The two independent toluene molecules also possess mirror symmetry. Figure 1 presents a perspective view of the molecule in which phenyl rings have been omitted. A second view, with phenyl rings, appears in Figure 2. A stereoview of the unit cell contents is given in Figure 3. Interatomic distances and angles are listed in Table IV.

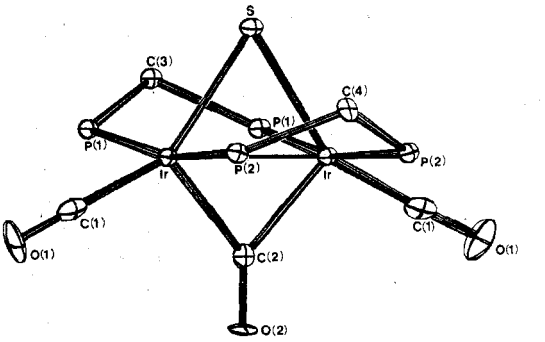

Figure 1. Perspective view of $[Ir_2(\mu\text{-}S)(\mu\text{-}CO)(CO)_2(dpm)_2]$. The phenyl rings have been omitted for clarity.

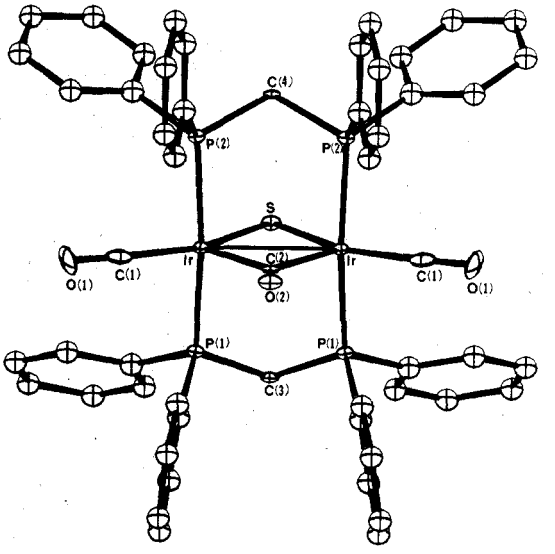

Figure 2. Perspective view of $[Ir_2(\mu\text{-}S)(\mu\text{-}CO)(CO)_2(dpm)_2]$ with phenyl rings.

The overall coordination geometry closely resembles two square-pyramidal coordinated iridium atoms which share a common apex at the bridging carbon monoxide. The approximately square-equatorial planes contain the two dpm phosphorus atoms, bridging sulfur, and terminal carbon monoxide, with trans angles P(1)–Ir–P(2) = 166.7 (1)° and S–Ir–C(1) = 151.5 (4)° and cis angles P(1)–Ir–S = 85.6 (1)°, P(2)–Ir–S = 87.1 (1)°, P(1)–Ir–C(1) = 90.9 (4)°, and P(2)–Ir–C(1) = 90.2 (4)°. The mean displacement of an atom from the square coordination planes containing S, C(1), P(1), and P(2) is 0.11 (19) Å. The iridium atom is displaced slightly (0.237 (2) Å) from the basal plane of ligands as in mononuclear square-pyramidal structures.[30,31] The bridging carbon monoxide exhibits a cis relationship to the four ligands in the plane (C(2)–Ir–S = 101.4 (3)°, C(2)–Ir–C(1) = 107.1 (5)°, C(2)–Ir–P(1) = 96.4 (4)°, C(2)–Ir–P(2) = 95.9 (4)°). The dihedral angle between the two square planes containing S, C(1), P(1), and P(2) and S, C(1)′, P(1)′, and P(2)′ is 97.0°.

(30) Cheng, C. H.; Spivack, B. D.; Eisenberg, R. *J. Am. Chem. Soc.* **1977**, *99*, 3003.
(31) Cheng, C. H.; Hendriksen, D. E.; Eisenberg, R. *J. Organomet. Chem.* **1977**, *142*, C65.

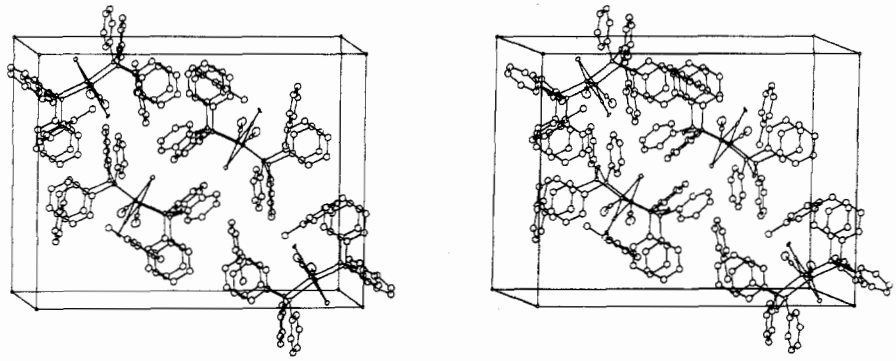

Figure 3. Stereoview of the unit cell of $[Ir_2(\mu\text{-}S)(\mu\text{-}CO)(CO)_2(dpm)_2]\cdot 2C_7H_8$.

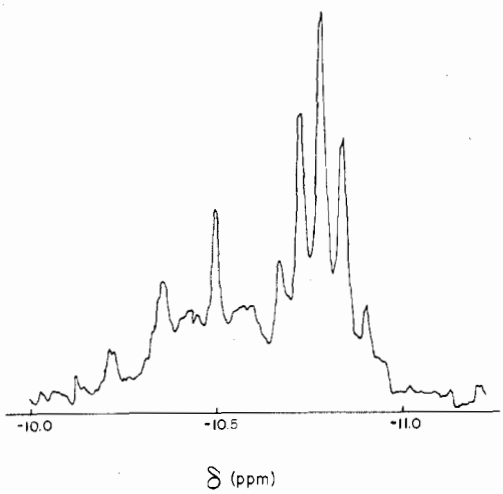

Figure 4. Upfield ^1H NMR spectrum of $[Ir_2H_2(\mu\text{-}S)(CO)_2(dpm)_2]$ after 1 h.

Table IV. Distances (Å) and Angles (Deg) of $[Ir_2(\mu\text{-}S)(\mu\text{-}CO)(CO)_2(dpm)_2]^a$

		Distances	
Ir-C(1)	1.80 (1)	P(1)-P(1)C(21)	1.825 (8)
Ir-C(2)	2.07 (1)	P(1)-P(1)C(11)	1.827 (8)
Ir-P(1)	2.322 (3)	P(2)-P(2)C(11)	1.820 (8)
Ir-P(2)	2.319 (3)	P(2)-P(2)C(21)	1.827 (7)
Ir-S	2.463 (3)	P(1)···P(1)	3.045 (6)
Ir-Ir	2.843 (2)	P(2)···P(2)	3.028 (6)
P(1)-C(3)	1.841 (8)	O(1)···P(1)H(26)	2.60 (2)
P(2)-C(4)	1.829 (8)	O(2)···P(1)H(16)	2.49 (1)
C(1)-O(1)	1.16 (1)	O(2)···P(2)H(22)	2.61 (1)
C(2)-O(2)	1.18 (2)	C(3)···P(1)H(22)	2.54 (2)
		Intermolecular Distances	
O(2)···P(1)H(24)	2.61 (1)	P(2)H(24)···P(2)H(25)	2.34 (2)
P(2)H(15)···P(2)H(15)	2.33 (2)		
		Angles	
C(1)-Ir-C(2)	107.1 (5)	Ir-S-Ir	70.5 (1)
C(1)-Ir-P(2)	90.2 (4)	C(3)-P(1)-Ir	114.4 (4)
C(1)-Ir-P(1)	90.9 (4)	C(4)-P(2)-Ir	110.7 (5)
C(1)-Ir-S	151.5 (4)	O(1)-C(1)-Ir	178 (1)
C(2)-Ir-P(2)	95.9 (4)	O(2)-C(2)-Ir	136.7 (3)
C(2)-Ir-P(1)	96.4 (4)	P(1)-C(3)-P(1)	111.6 (7)
C(2)-Ir-S	101.4 (3)	P(2)-C(3)-P(2)	111.7 (7)
P(2)-Ir-P(1)	166.7 (1)	Ir-C(2)-Ir	86.7 (6)
P(2)-Ir-S	87.1 (1)		
P(1)-Ir-S	85.6 (1)		

[a] Dihedral angle between least-squares planes [S, P(1), P(2), C(1) C(1)] and [S, P(1)', P(2)', C(11)'] is 97.0°. Angle between vector P(1)-P(2) and plane [Ir, S, C(1)] is 89.4 (2)°.

The trans dpm phosphorus atoms, P(1) and P(2), are essentially normal to a plane containing the metal atoms and all other ligands in the complex. The positions of the two iridium, bridging sulfur, and carbon and oxygen atoms of the three carbon monoxides do not deviate by more than 0.01 Å from their least-squares plane. The angle between the P(1)-P(2) vector and this plane is 89.4 (2)°. The structure can be considered to result from the addition of CO to two square-planar Ir(I) ions of the $[Ir_2(\mu\text{-}S)(CO)_2(dpm)_2]$ A-frame skeleton. The locally square-pyramidal product $[Ir_2(\mu\text{-}S)(\mu\text{-}CO)(CO)_2(dpm)_2]$ shows a bridging carbonyl in an apical arrangement to the original square planes of ligands. The total structure is similar to two cationic endo CO rhodium A-frame adducts, $[Rh_2(\mu\text{-}Cl)(\mu\text{-}CO)(CO)_2(dpm)_2]^+$ and $[Rh_2(\mu\text{-}H)(\mu\text{-}CO)(CO)_2(dpm)_2]^+$.

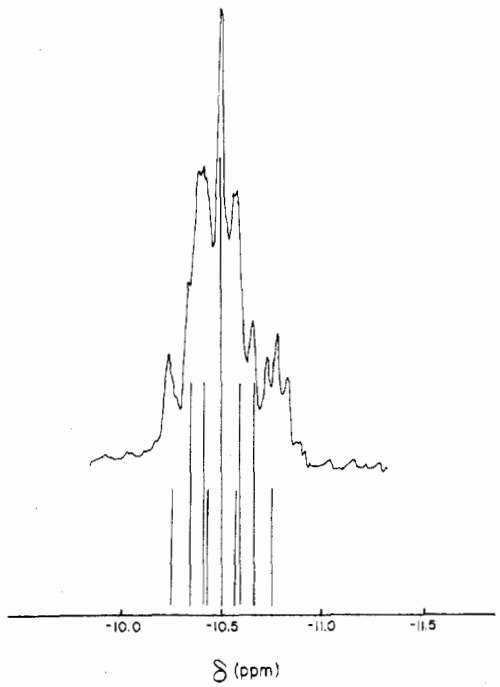

Figure 5. Upfield ^1H NMR spectrum of $[Ir_2H_2(\mu\text{-}S)(CO)_2(dpm)_2]$ after 12 h and an idealized triplet of triplets on the assumption that $^2J_{PH} = 16.1$ Hz and $^3J_{PH} = 9.0$ Hz.

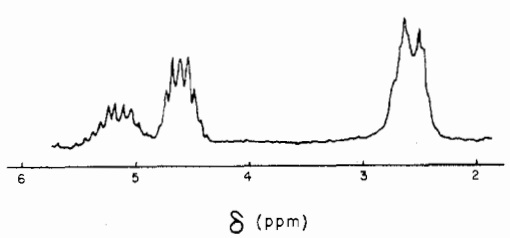

Figure 6. ^1H NMR spectrum of the dpm methylene region for the two $[IrH_2(\mu\text{-}S)(CO)_2(dpm)_2]$ isomers. Each species exhibits a separate resonance at δ 5.16 and 4.59 for one of the methylene protons and overlapped resonances at $\delta \sim 2.57$ for the second protons. The $^1H\{^{31}P\}$ NMR spectrum shows doublets at δ 5.16 ($^2J_{P-H} = 12$ Hz) and 4.59 ($^2J_{P-H} = 14$ Hz) and two overlapped doublets at $\delta \sim 2.57$.

The bonding distances in the structure (Table IV) appear normal. The Ir–Ir separation (2.843 (2) Å) is slightly longer than the mean distance of ca. 2.76 Å[32,33] found in polynuclear iridium cluster compounds but is consistent with an Ir–Ir single bond. The Ir–Ir single bond gives an 18-e configuration to each of the two metal centers. The compression along the Ir–Ir internuclear axis is evident in a shorter separation between the metals than between adjacent dpm phosphorus atoms (P(1)···P(1)′ = 3.045 (6), P(2)···P(2)′ = 3.028 (6) Å). The bridging sulfur exhibits both a longer bond distance (Ir–S = 2.463 (3) Å) and narrower bond angle (Ir–S–Ir = 70.5 (1)°) to the metal centers than the rhodium sulfide A frame, $[Rh_2(\mu\text{-}S)(CO)_2(dpm)_2]$ (Rh–S = 2.367 (3) Å, Rh–S–Rh = 83.5 (1)°).[3] The narrower M–S–M angle is attributed to the compression along the Ir–Ir bond (2.843 (2) Å) compared to the nonbonding Rh···Rh distance of 3.154 (2) Å. A similar trend is seen in the Rh–Cl–Rh bond angle and distances in the rhodium chloride A-frame cation, $[Rh_2(\mu\text{-}Cl)(CO)_2(dpm)_2]^+$, and its endo carbonyl adduct, $[Rh_2(\mu\text{-}Cl)(\mu\text{-}CO)(CO)_2(dpm)_2]^+$.[5,8]

The two Ir–P bond lengths of 2.322 (3) and 2.319 (3) Å are identical within experimental error and agree with those reported for other iridium phosphine complexes.[34–36] Similarly, the Ir–C distances for both the terminal (1.80 (1) Å) and bridging carbonyls (2.07 (1) Å) correspond to reported values.[32] The P–C bond lengths in the dpm ligand range from 1.820 (8) to 1.841 (8) Å and are typical for dpm complexes.[3,5,6,8,12]

There are no unusual intra- or intermolecular nonbonded contacts in the structure. The solvent toluene molecules are well separated from the $[Ir_2(\mu\text{-}S)(\mu\text{-}CO)(CO)_2(dpm)_2]$ molecule and appear to have no other role than filling space in the lattice. The closest intermolecular phenyl hydrogen contacts are P(2)H(15)···P(2)H(15) = 2.33 (2) and P(2)H(24)···P(2)H(25) = 2.34 (2) Å. All other phenyl H···H distances in the structure are greater than the sum of van der Waals radii (2.4 Å). A partial tabulation of nonbonded distances is given in Table IV.

Summary and Conclusions

The iridium A-frame complex, $[Ir_2(\mu\text{-}S)(CO)_2(dpm)_2]$, shows much greater reactivity than its rhodium analogue with CO and H_2. The carbonyl adduct, which has been structurally characterized, shows attachment of the addend molecule in the pocket of the A frame on the endo side of the molecule. Oxidative addition of H_2 to the original iridium complex leads to the formation of two different adducts which are characterized by ^1H NMR spectroscopy. The NMR data suggest that in one of the hydride species the added H_2 also resides on the endo side of the complex. The iridium complex also shows greater reactivity than its rhodium analogue by acting as a hydrogenation catalyst with simple unsaturated substrates. Extensions to other potential reduction substrates are under investigation.

Acknowledgment. We wish to thank the National Science Foundation (Grant CHE76-17440) and the donors of the Petroleum Research Fund, administered by the American Chemical Society, for support of this research. A generous loan of precious metal salts from Matthey Bishop Co., Inc., is also gratefully acknowledged. C.P.K. wishes to acknowledge an Elon Huntington Hooker Fellowship and a Sherman Clarke Fellowship. The experimental assistance of Mr. Yukio Kuroda in the NMR studies is most appreciated.

Registry No. $Ir_2(\mu\text{-}S)(\mu\text{-}CO)(CO)_2(dpm)_2 \cdot 2C_6H_5CH_3$, 73972-10-8; $[Ir_2Cl(CO)_4(dpm)_2]^+[IrCl_2(CO)_2]^-$, 73972-11-9; $[Ir_2Cl(CO)_4(dpm)_2]^+PF_6^-$, 73972-12-0; $Ir_2(\mu\text{-}S)(CO)_2(dpm)_2$, 73972-13-1; $Ir_2(\mu\text{-}S)(BF_3)(CO)_2(dpm)_2$, 73972-14-2; $Ir_2H_2(\mu\text{-}S)(CO)_2(dpm)_2$ (hydride species I), 73972-15-3; $Ir_2H_2(\mu\text{-}S)(CO)_2(dpm)_2$ (hydride species II), 74033-51-5; $Ir_2Cl_2(1,5\text{-}COD)_2$, 12112-67-3.

Supplementary Material Available: A listing of observed and calculated structure factor amplitudes (10 pages). Ordering information is given on any current masthead page.

(32) Pierpont, C. G.; Stuntz, G. F.; Shapley, J. R. *J. Am. Chem. Soc.* **1978**, *100*, 616; *Inorg. Chem.* **1978**, *17*, 2596.
(33) Shapley, J. R.; Stuntz, G. F.; Churchill, M. R.; Hutchinson, J. P. *J. Am. Chem. Soc.* **1979**, *101*, 7425.
(34) Clark, G. R.; Collins, T. J.; James, S. M.; Roper, W. R.; Town, K. G. *J. Chem. Soc., Chem. Commun.* **1976**, 475.
(35) Hodgson, D. J.; Ibers, J. A. *Inorg. Chem.* **1969**, *8*, 1232.
(36) Brock, C. P.; Ibers, J. A. *Inorg. Chem.* **1972**, *11*, 2812.